Vol 17 No 8, August 2008
1674-1056/2008/17(08)/3077-06

Chinese Physics B

© 2008 Chin. Phys. Soc.
and IOP Publishing Ltd

Quantum compact model for thin-body double-gate Schottky barrier MOSFETs*

Luan Su-Zhen(栾苏珍)[a)b)†] and Liu Hong-Xia(刘红侠)[a)b)]

[a)] *School of Microelectronics, Xidian University, Xi'an* 710071, *China*
[b)] *Key Laboratory of Ministry of Education for Wide Band-Gap Semiconductor Materials and Devices, Xi'an* 710071, *China*

(Received 30 August 2007; revised manuscript received 12 March 2008)

Nanoscale Schottky barrier metal oxide semiconductor field-effect transistors (MOSFETs) are explored by using quantum mechanism effects for thin-body devices. The results suggest that for small nonnegative Schottky barrier heights, even for zero barrier height, the tunnelling current also plays a role in the total on-state current. Owing to the thin body of device, quantum confinement raises the electron energy levels in the silicon, and the tradeoff takes place between the quantum confinement energy and Schottky barrier lowering (SBL). It is concluded that the inclusion of the quantum mechanism effect in this model, which considers an infinite rectangular well with a first-order perturbation in the channel, can lead to the good agreement with numerical result for thin silicon film. The error increases with silicon thickness increasing.

Keywords: Schottky barrier, quantum mechanism effects, effective mass, electron density
PACC: 7340Q, 0365, 7110C, 7125J

1. Introduction

The symmetric ultrathin-body double-gate (UTBDG) metal oxide semiconductor field-effect transistors (MOSFET) is considered to be one of the most promising candidates for sub-30 nm MOSFET. Because of its good short-channel behaviour, low leakage, small subthreshold swing, and scalability better than that of a bulk MOSFET, it has become an intense subject of transistor research. Recently, there has been much progress toward an understanding of the physics of double-gate devices, deriving many analytical models.[1−3] More and more experimental results demonstrate the practicality of such devices.[4−6] However, in the UTBDG devices with doped source/drain, a tradeoff between series resistance and fringing capacitance places tight restriction on device gate heights and also leads to performance degradation. UTBDG devices with metal source/drain do not suffer this tradeoff because the resistivity of metals is two orders of magnitude smaller than that of heavily doped silicon. This paper investigates the possibility of replacing doped source/drain with metal source/drain in UTBDG devices. Theoretical studies of Schottky barrier (SB) devices have focused on assessing device operation on a nanometre scale, treating the tunnelling through SBs between metal source/drain and silicon, and fitting the experimental data.[7,8] However, they all focus on electrostatic analysis, thus ignoring quantum mechanism (QM) effects that are indispensable in a decananoscale range. For a thin body device, quantum confinement raises the electron energy levels in the silicon, so that the effective barrier height turns large. Then several questions remain to be solved. For example, how does Schottky barrier height (SBH) varies with the quantum confinement? For low barrier heights, what plays a dominant role in total on-state current, tunnelling current or thermionic current? In this paper, we address these questions by analytically describing the eigen-energy levels in ultrathin-body double-gate Schottky barrier MOSFET (UTBDGSBMOSFET). Then, an implicit expression for electron density and a closed form of on-state current for UTBDGSBMOSFET are presented by considering the QM effects. The analytical values of eigen-energy levels, electron

*Project supported by the National Natural Science Foundation of China (Grant No 60206006), the Program for New Century Excellent Talents of Ministry of Education of China (Grant No NCET-05-085) and the Xi'an Applied Materials Innovation Fund (Grant No XA-AM-200701).
†E-mail: szluan@mail.xidian.edu.cn

densities, and on-state currents with arbitrary device parameters are in good agreement with the numerical results.

2. Drain current modelling

2.1. Analytical description of eigenenergies

Figure 1(a) shows the schematic of a symmetric UTBDGSBMOSFET and Fig.1(b) gives the band diagrams in horizontal cross-section, together with the first energy subbands. With the assumption of an infinite rectangular well in the channel (ignoring the non-uniform potential) and infinitely high potential barriers at the silicon/oxide interfaces along the y-direction, the following analytical expression of energy level, $E_{i,j}$, is derived as

$$E_{i,k_\mathrm{squ}} = \frac{\hbar^2\pi^2 i^2}{2qm_k^* t_{\mathrm{Si}}^2}, \tag{1}$$

where i is the quantum number, k refers to different valleys of the silicon conduction band, and m_k^* is the effective mass along the y-direction of valley k with $m_1^* = m_{\mathrm{l}}^* = 0.98m_0$ and $m_2^* = m_{\mathrm{t}}^* = 0.19\,m_0$ with subscript 1 referring to unprimed valley and subscript 2 referring to primed valley for a silicon with $< 100 >$ crystal orientation, m_{l}^* is the longitudinal mass, m_{t}^* the transverse mass, and m_0 the free electron mass. This formula, however, is not sufficiently correct with a high gate bias because the nonuniformity of the electric potential along the y-direction cannot be neglected. Therefore, the first-order correction to the energy levels by using the time-independent perturbation theory is carried out, with a perturbation energy δE_{i} being $< \varphi_i\,|\delta H\,|\varphi_i >$, where δH is the Hamiltonian of the perturbation and $\delta H = -q^2 n_{\mathrm{e}} y^2/2\varepsilon_{\mathrm{Si}}$, φ_{i} is the electron wave function related to energy level $E_{i,k}$. Thus, we find first-order correction as shown in Ref.[9]

$$\delta E_i = -\frac{q^2 n_{\mathrm{e}} t_{\mathrm{Si}}^2}{24\varepsilon_{\mathrm{Si}}}\left[1 - \frac{6}{(\pi i)^2}\right]. \tag{2}$$

So the analytical results $E_{i,k}$ with first-order perturbation can be expressed as

$$E_{i,k} = E_{i,k_\mathrm{squ}} + \delta E_i. \tag{3}$$

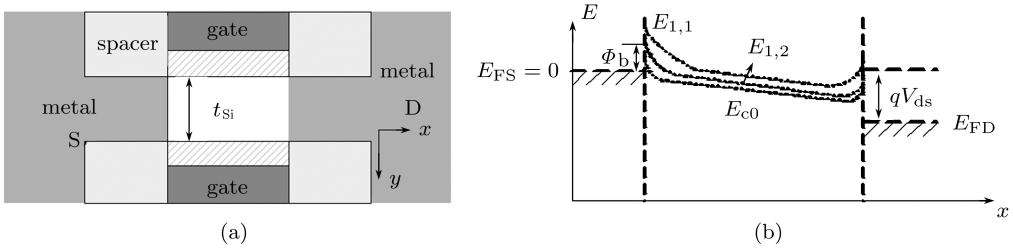


Fig.1. Schematic symmetrical UTBDGSBMOSFET structure (a) and the band diagram in a horizontal cross-section of a channel (b).

2.2. Quantum inversion charge

Owing to the confinement of electron motion normal to the interface, the conduction band within the transistor channel is split into several subbands, and each of them is associated with the corresponding energy eigenvalue. Hence, the electron density in the channel may be expressed as

$$n_{\mathrm{e}} = \sum_{i=1}^{N_{\mathrm{t}}}\sum_{k=1}^{N_{\mathrm{m}}} g_k N_k \ln\left\{1 + \exp\left(\frac{E_{i,k} - E_{\mathrm{c0}}}{k_{\mathrm{B}}T}\right) \times \exp\left[\frac{q(\phi_{\mathrm{c}} - \phi_{\mathrm{Fn}})}{k_{\mathrm{B}}T}\right]\right\}, \tag{4}$$

where $N_k = (m_{\mathrm{dk}}^* k_{\mathrm{b}} T/\pi\hbar^2)$ is the density of states in the subband at energy $E_{i,k}$ with $\hbar$ being the reduced Plank's constant, and m_{dk}^* being the density of states effective mass ($m_{\mathrm{d1}}^* = m_{\mathrm{t}}^*$ and $m_{\mathrm{d2}}^* = (m_{\mathrm{l}}^* m_{\mathrm{t}}^*)^{1/2}$); $N_{\mathrm{t}} = 6$ is the number of subbands; $N_{\mathrm{m}} = 2$ is the number of different sets of valleys; $g_1 = 2$ and $g_2 = 4$ that are the degeneracy of the valleys of set; $\phi_{\mathrm{c}} = -E_{\mathrm{c0}}/q$; $\phi_{\mathrm{Fn}} = -E_{\mathrm{Fn}}/q$ with E_{c0} and E_{Fn} being the central point value of potential well and the quasi-Fermi level, respectively; k_{B} is the Boltzmann constant; and T is the temperature. On the other hand, according to 1D electrostatic analysis, the electron density may be also expressed as[9]

$$n_{\mathrm{e}} = 2C_{\mathrm{g}}(V_{\mathrm{G}}' - \phi_{\mathrm{c}})/q, \tag{5}$$

where $C_g = C_{ox}C_d/(C_{ox}+C_d)$ represents the gate capacitance per unit area with $C_{ox} = \varepsilon_{ox}/t_{ox}$ being the oxide capacitance per unit area and $C_d = 4\varepsilon_{Si}/t_{Si}$ being the depletion capacitance per unit area; $V'_G = V_G - (\phi_M - \chi)$ is the effective gate voltage with V_G being the gate bias, ϕ_M being the work function of the gate material, and χ being the electron affinity of the semiconductor.

2.3. Drain current modelling

In a UTBDG device with metal S/D, we consider two major transport mechanisms through the Schottky contacts: thermionic emission and barrier tunnelling ($J = J_{therm} + J_{tun}$) expressed respectively as

$$J_{therm} = \frac{A^*T}{k_B}\int_{E_{c0}+q(\phi_i-V_a-\Delta\phi_b)}^{\infty}[f_s(E_{i,k}\pm q\Delta\phi_b) - f_d(E_{i,k}\pm q\Delta\phi_b)]\mathrm{d}E_{i,k}, \quad (6)$$

and

$$J_{tun} = \frac{A^*T}{k_B}\int_{E_{c0}}^{E_{c0}+q(\phi_i-V_a-\Delta\phi_b)} \times T_t(E_{i,k})[f_s(E_{i,k}\pm q\Delta\phi_b) - f_d(E_{i,k}\pm q\Delta\phi_b)]\mathrm{d}E_{i,k}, \quad (7)$$

where $q\phi_i = q\phi_{b0} - (E_{c0} - E_{Fn})$, with E_{c0} being the conduction band edge energy deep inside the silicon, ϕ_{b0} being the SBH, and ϕ_i being the build-in potential at zero contact bias; V_a is the forward bias across the Schottky contact; $T_t(E_{i,k})$ is the transmission coefficient; A^* is the effective Richardson's coefficient ($112A/\mathrm{cm}^2\cdot\mathrm{K}^2$ for electrons and 32 for holes in silicon); $f_s(E_{i,k}) = \dfrac{1}{1+\exp\left(\dfrac{E_{i,k}-E_{Fn}}{k_BT}\right)}$ and $f_d(E_{i,k}) = \dfrac{1}{1+\exp\left(\dfrac{E_{i,k}-E_{Fn}+qV_a}{k_BT}\right)}$ are the Fermi–Dirac (F-D) distributions at the source and the drain, respectively. As a factor affecting the electrical transport, the Schottky barrier lowering (SBL) due to the image force effect and the interfacial film is also considered in our study, which is given by the following expression:

$$\Delta\phi_b = \sqrt{\frac{q\alpha E_S}{4\pi\varepsilon_s}} + \eta E_S, \quad (8)$$

where E_S is the maximum lateral field at the Schottky contact, which can be expressed as

$$E_S = \frac{\phi_b - \phi_n + V_a}{W_b}, \quad (9)$$

with $W_b = \sqrt{2\varepsilon_{Si}(\phi_b - \phi_n + V_a)/qn_e}$ being the width of SB and $\phi_n = k_BT\ln(N_C/n_e)$.

The first term in expression (8) describes the SBL due to the image force; the second term is generated by the interfacial film. α is a fitting parameter. Classical theory sets it to be one;[10] however, fitting this model to empirical data suggests that this value depends on V_{DS} and L_g. The value of η usually is set to be 1.5–3 nm, here it is set to be 1.5 nm. N_C is the density of states in the first subband.

Since $\Delta\phi_b$ causes a shift in both the electron and hole barrier heights, this is equivalent to an energy shift of the entire band gap relative to the Fermi level in the metallic S/D regions. This can be expressed mathematically by shifting the F–D distributions in the S/D regions by $\Delta\phi_b$ (positive for electrons, negative for holes). For the calculation by using the model, rather than integrating expressions (6) and (7) over an energy range, a Riemann sum over a fine energy grid ($\Delta E = 0.001$ to 0.01 eV) is used. Also, instead of using ∞ as the final energy in expression (6), a finite value between one and three (depending on V_{ds}) is equally useful, as the tail of the F–D distribution becomes very small quickly. Furthermore, V_{ds} must also be included to account for the difference in F–D distribution between the source and the drain at a given energy.

A nonlocal tunnelling model is employed based on the F–D distribution function in our model, and the tunnelling probability based on the Wentzel–Kramers–Brillouin (WKB) approximation is

$$T_t(E_{i,k}) = \exp\left\{\frac{2}{\hbar q}\sqrt{\frac{m_k^*\varepsilon_{Si}}{n_e}}\left[E_{i,k}\ln\left(\frac{\sqrt{E_b}+\sqrt{E_b-E_{i,k}}}{\sqrt{E_{i,k}}}\right) - \sqrt{E_b}\sqrt{E_b-E_{i,k}}\right]\right\}, \quad (10)$$

where $E_{\rm b} = E_{\rm c0} + q(\phi_{\rm i} - V_{\rm a} - \Delta\phi_{\rm b})$. The effective mass in the above equation is anisotropic for electrons, which brings anisotropy to the tunnelling current of electrons. Silicon contains six conduction band minima located at the Δ points in the first Brillouin Zone. In the $< 100 >$ direction, two of the conduction band minima each have an electron effective mass of $0.98\,m_0$, and four of them each have an electron effective mass of $0.19\,m_0$. The tops of valence bands are nearly isotropic. Light holes each have an effective mass of $0.16\,m_0$, and heavy holes each have an effective mass of $0.2\,m_0$ and a split-off energy of 44 meV. Tunnelling current is sensitive to the effective mass in expression (10). An accurate experimental determination of the tunnelling effective mass is thus important. Unfortunately, reliable experimental data of carrier tunnelling effective masses for nanoscale contacts with a wide range of barrier heights are not available. We calculate the tunnelling current based on the following assumptions: the tunnelling current through an SB is dominated by electrons and holes with light masses because their tunnelling probabilities are much larger as expected from expression (10).

3. Results and discussion

The validation procedure is continued by performing an in-depth investigation of the model capability to take into account the carrier quantization effects. For this purpose different energy levels ($i = 1, 2$) of different valleys ($k = 1, 2$) are depicted against silicon thickness in Fig.2. It is seen clearly from the figure that when the channel is narrow, the analytical solutions with the assumption of an infinite rectangular well plus the first-order perturbation correction accord well with the numerical results from the 2-dimensional device simulator ISE. However, with the thicknesses of silicon film being beyond 10 nm, the error between these two results becomes intolerant due to the quantum effects insignificant.

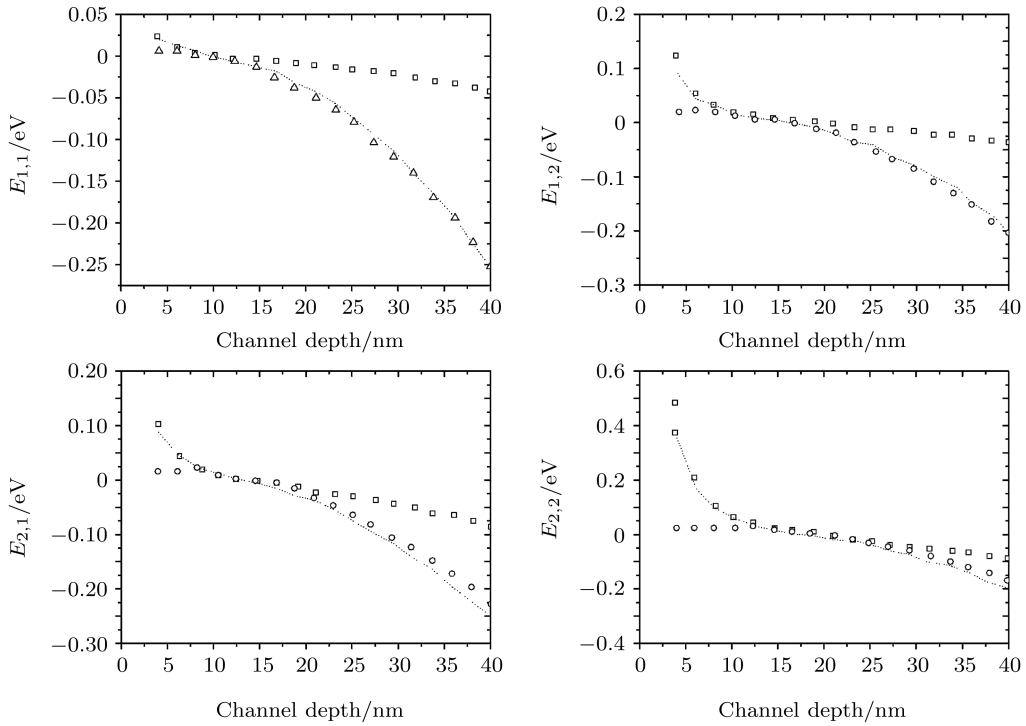


Fig.2. Energy levels E versus channel depth, where the squares represent analytical results $E_{i,k}$ with first-order perturbation, circles denote analytical results $E_{i,k}$ and dash lines refer to numerical results.

In Fig.3, the analytical charge densities are depicted against gate voltage for different thicknesses of silicon film ($t_{\rm Si}$), which are in good agreement with the numerical simulation results. According to our model, the electron density increases with $t_{\rm Si}$ scaling down in a subthreshold region while it becomes independent of $t_{\rm Si}$ under a high gate voltage. Considering the first-order perturbation, the results from

our model are consistent well with numerical results while the assumption of rectangular well leads to a considerable overestimate of the values and the error becomes larger with t_{Si} decreasing. Further calculations of drain current with and without QM effects for the S/D SBs are shown in Fig.4 (the gate workfunction for this device has been selected to produce an off-state current of $1\,\mathrm{nA}/\mu\mathrm{m}$). Note that the 2D QM model perfectly reproduces two essential phenomena: the quantum effect on drain current is increasingly significant as t_{Si} is scaled down; the drain current dependence on t_{Si} in the subthreshold region, above threshold drain current, depends much less on t_{Si}.

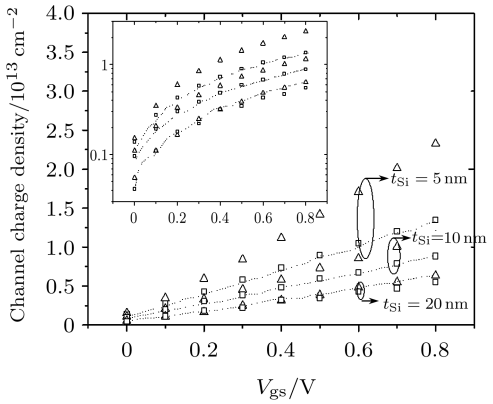


Fig.3. The analytical charge densities against gate voltage for different thicknesses of silicon film (t_{Si}).

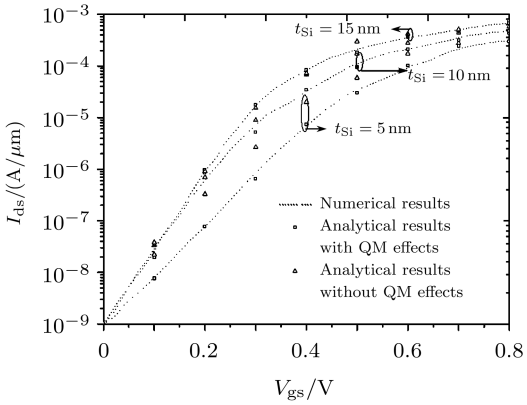


Fig.4. Effect of silicon film thickness on the drain current for 20 nm UTBDGSBMOSFET.

Figure 5 compares the first subband profiles of these SBMOSFETs under on-state conditions beyond a certain gate voltage. It is somewhat of a surprise, that a tunnelling barrier still exists for $\phi_{\mathrm{b0}} = 0\,\mathrm{eV}$. The current of the SBMOSFETs with a zero effective barrier height is limited by the tunnelling barrier at the source rather than by the thermomic barrier in the channel. For this thin body device, quantum confinement raises the electron energy levels in the silicon, so that the effective barrier height become large.

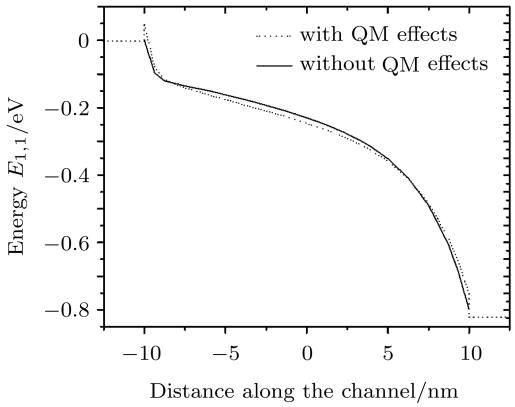


Fig.5. The energy band diagrams of a 20nm UTBDGSBMOSFET with SBH being zero at $V_{\mathrm{gs}} = V_{\mathrm{ds}} = 0.8\,\mathrm{V}$.

Figure 6 shows the energy band of an SBMOSFET in either on-or off-states with an SBH of $\phi_{\mathrm{b0}} = 0.56\,\mathrm{eV}$ comprising QM effects. When the device is off, the energy band resembles that of a conventional MOSFET with a large energy barrier between source and drain, and the current is limited by thermonic emission over the barrier at the source. On the drain side, the SB for holes is thin, which allows holes to tunnel from the drain terminal into the channel, thereby causing an extra leakage current. It can be concluded that the off-state current is composed of either thermionic or tunnelling components, depending on the gate work function and bias. Under a higher gate bias, a conduction band spike appears at the source. The SB of electrons on the source side is thin which allows electrons to tunnel from the source terminal into the channel. We also see that the barriers are thicker in the centre of the channel. The SBL (not shown in Fig.6) is also smaller in the centre of the channel. Thus, the favourable path for tunnelling current is near the surface rather than through the centre of the channel. The lower the SB is for electrons, the higher the SB will be for holes. As a result, the tunnelling current of holes decreases. This explains the reduced hole for lower electron SB in Fig.7. The minimum leakage current is insensitive to SBH. It is the consequence of a tradeoff between the electron current and the hole current. It is interesting to note that the minimum leakage currents for the zero barrier and the mid gap SBMOSFETs are similar. The reason for this can be explained as follows: the gate oxide ($t_{\mathrm{ox}} = 1\,\mathrm{nm}$) used in our model is very thin, and

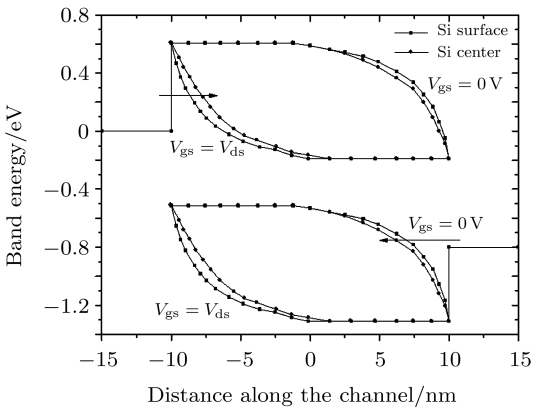


Fig.6. Conduction and valence bands from source to drain for a UTBDGSBMOSFET.

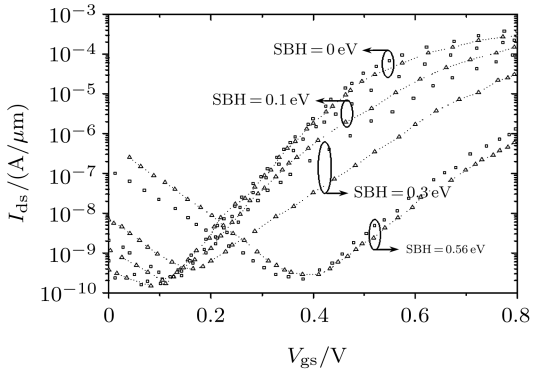


Fig.7. I_{ds}-V_{gs} curves for UTBDGSBMOSFETs with different LBHs for electrons.

the SB is also very thin and essentially transparent to carriers. The current is, therefore, limited by thermionic emission over a barrier of which the height is determined by the conduction/valence band in the interior of the channel. Tunnelling through the metal/semiconductor barrier varies with the barrier height and the bias, but it can play a minor role (because the barrier is so transparent) compared with the barrier in the silicon body. Above the threshold, the situation is different. The tunnelling resistance restricts the on-state current; the zero barrier delivers more on-current. Moreover, as shown in Fig.7, the analytical solutions fully comprising QM effects with the first-order perturbation are in good agreement with the numerical results. The model merely with SBL overestimates the value of the drain current.

4. Conclusions

A short channel quantum compact model for drain current in thin-body double-gate SBMOSFETs has been developed. For thin body devices, quantum confinement raises the electron levels in the silicon, so that the effective barrier height becomes large. The previous studies merely included the SBL in their models either ignoring QM effects or making too coarse assumptions of the quantum potential well, which leads to an overestimate of the drain current. The starting point of developing our model is to take into consideration the analytical solutions to energy levels with the first-order perturbation. According to our model, the current of the SBMOSFETs with zero effective barrier heights involves the tunnelling current due to quantum confinement. No matter what the barrier heights are, the minimum leakage currents are similar due to the thin gate oxide. Beyond the threshold, the lower SBH delivers more on-state current. The numerical results validate the proposed model. The analytical solutions can provide additional insights into the new physical phenomenon.

References

[1] Taur Y 2000 *IEEE Electron Device Lett.* **21** 245

[2] Wang C, Snyder J P and Tucker J R 1999 *Appl. Phys. Lett.* **74** 1174

[3] Rhoderick E H and Williams R H 1988 *Metal–Semiconductor Contacts* (Oxford, UK: Clarendon) p86

[4] Taur Y and Ning T H 1998 *Fundamentals of Modern* VLSI *Devices* (Cambridge: Cambridge University Press) p469

[5] Pellegrini B 1976 *J. Phys.* D: *Appl. Phys.* **9** 55

[6] Xiong S Y, King T J and Bokor J 2005 *IEEE Trans. Electron Device* **52** 185

[7] Huang C K, Zhang W E and Yang C H 1998 *IEEE Trans. Electron Devices* **45** 842

[8] Winstead B and Ravaioli U 2000 *IEEE Trans. Electron Devices* **47** 1241

[9] Baccarani G and Reggiani S 1999 *IEEE Trans. Electron Devices* **46** 1656

[10] Pierret R F 1996 *Semiconductor Device Fundamentals* (Reading, MA: Addison-Wesley) p492